

A. D. Freed · K. Diethelm

Fractional calculus in biomechanics: a 3D viscoelastic model using regularized fractional derivative kernels with application to the human calcaneal fat pad

Received: 26 May 2005 / Accepted: 30 November 2005 / Published online: 31 March 2006
© Springer-Verlag 2006

Abstract A viscoelastic model of the K-BKZ (Kaye, Technical Report 134, College of Aeronautics, Cranfield 1962; Bernstein et al., *Trans Soc Rheol* 7:391–410, 1963) type is developed for isotropic biological tissues and applied to the fat pad of the human heel. To facilitate this pursuit, a class of elastic solids is introduced through a novel strain-energy function whose elements possess strong ellipticity, and therefore lead to stable material models. This elastic potential – via the K-BKZ hypothesis – also produces the tensorial structure of the viscoelastic model. Candidate sets of functions are proposed for the elastic and viscoelastic material functions present in the model, including two functions whose origins lie in the fractional calculus. The Akaike information criterion is used to perform multi-model inference, enabling an objective selection to be made as to the best material function from within a candidate set.

Dedicated to Prof. Ronald L. Bagley.

A. D. Freed (✉)
Bio Science & Technology Branch, MS 49-3,
NASA's John H. Glenn Research Center at Lewis Field,
21000 Brookpark Road,
Cleveland, OH 44135, USA
E-mail: Alan.D.Freed@nasa.gov

A. D. Freed
Department of Biomedical Engineering, ND-20,
The Cleveland Clinic Foundation,
9500 Euclid Avenue,
Cleveland, OH 44195, USA

K. Diethelm
GNS Gesellschaft für Numerische Simulation mbH,
Am Gaußberg 2,
38114 Braunschweig, Germany
E-mail: Diethelm@gns-mbh.com

K. Diethelm
Institut Computational Mathematics,
Technische Universität Braunschweig,
Pockelsstraße 14,
38106 Braunschweig, Germany

1 Introduction

The human heel is comprised of skin, a fat pad, the origin of the plantar aponeurosis tendon and the calcaneal bone. Collectively, the soft tissues therein constitute the heel pad. The heel pad is our body's natural shock absorber, dissipating impulses introduced into the body during normal activity, and thereby attenuating the forces that are transmitted up through the body's skeletal structure (Cavanagh et al. 1984).

NASA has a need to understand how much force is being transferred into the load-bearing bones of the body during exercise so that effective countermeasure protocols can be developed to help avert bone loss in astronauts during long space missions (Lang et al. 2004). Current devices that measure in-shoe forces beneath the heel have recorded forces that exceed twice the body weight when an astronaut ran on a treadmill on Earth; whereas, when running on an identical treadmill located within the International Space Station, using the same in-shoe transducers and a harness attached at the waist pushing the astronaut against the treadmill, maximum forces of about one and one-half times the body weight were recorded (Cavanagh et al. 2005). To determine the impact force that is actually being transmitted to bone will require numerical analysis. To be able to run such an analysis will require material models for the soft-tissue constituents of the heel pad. Here we develop a viscoelastic material model for the human calcaneal fat pad.

Although the fractional calculus¹ has enjoyed wide application in synthetic polymer rheology (see Podlubny 1999, pp. 268–277, for a brief literature review), it has attracted limited attention in the field of biomechanics: Suki et al. (1994) found the pressure/volume response of a whole lung to be aptly characterized by a Newtonian fractional-order viscoelastic (FOV) material model with a fractional order of

¹ Calculus is the study of properties of functions in one or more variables, using derivatives and integrals. Fractional calculus extends the classic study of integer-order derivatives and integrals to include derivatives and integrals of non-integer order, e.g., $d^{\alpha}y/dx^{\alpha}$.

evolution of 0.1;² his colleagues, Yuan et al. (1997, 2000), studied lung tissue and found its fractional order of evolution to be about the same, viz., 0.075; while Chen et al. (2004) applied the same model to agarose gels used for culturing tissues, especially cartilage, and found its value to be about 0.03. These are all values close to that of ideal elasticity, where the order of evolution is 0. In a study of charge dynamics in protein molecules, Glöckle and Nonnenmacher (1995) derived a kinetic equation in the form of a fractional-order integral equation (i.e., a Volterra equation of the second kind with an Abel power-law kernel) and found the charge relaxation in myoglobin to be accurately described by a formula where the fractional order of evolution was set at -0.4 .³ In papers by Carew et al. (2003) and Doehring et al. (2004), the response of aortic heart valves to 1D experiments has been shown to be well represented by a quasi-linear⁴ Kelvin–Zener FOV solid with the fractional order of evolution being about 0.25.

In this paper, we present a K-BKZ viscoelastic model tailored to the response of the human calcaneal fat pad loaded in compression. The paper begins with a presentation of the kinematic fields needed to construct such a theory. A novel class of nonlinear elastic solids that has great potential in the modeling of soft tissues is then presented. The K-BKZ hypothesis employs the elastic strain-energy function to establish the tensorial structure of the viscoelastic model. Four elastic functions and five viscoelastic kernel functions are considered as candidate models. The Akaike information criterion (AIC) information theoretic (Burnham and Anderson 2002) is used to select the ‘best’ models for these two material functions based on the compression and stress-relaxation experiments of Miller–Young et al. (2002). A power law is found to be the best model for the elastic part of the response, and a regularized fractional derivative (RFD) is found to be the best viscoelastic kernel.

2 Kinematics

Consider a rectangular Cartesian coordinate system with orthonormal base vectors \mathbf{e}_1 , \mathbf{e}_2 and \mathbf{e}_3 . We focus our attention on a mass point originally located by the set of coordinates $\mathbf{X} = (X_1, X_2, X_3)$ assigned at an arbitrary reference time t_0 in this coordinate frame. At current time t , this

² For the Newtonian FOV model, a fractional order of evolution equaling 1 is the limiting case of a viscous Newtonian fluid, while a fractional order of evolution equaling 0 is the limiting case of an elastic Hookean solid.

³ Fractional-order integration and differentiation can be defined as a single operator that is continuous over the order parameter; hence, the term differ-integration (Oldham and Spanier 1974). The accepted notation employs a minus sign (e.g., -0.4) when designating the order of integration, and a plus sign (e.g., 0.4) when designating the order of differentiation.

⁴ A viscoelastic model is said to be ‘quasi-linear’ if: the linear strain (or forcing function) of classic (linear) viscoelasticity is replaced by a nonlinear strain measure, the kernel (or memory) function depends solely on time (i.e., strain-time separability applies), and only a onefold integral over time appears in the model. K-BKZ models are quasi-linear.

mass element is located by a different set of coordinates $\mathbf{x} = (x_1, x_2, x_3)$ in the same coordinate frame, while at some intermediate time – say s , $t_0 \leq s \leq t$ – it had coordinates $\boldsymbol{\chi} = (\chi_1, \chi_2, \chi_3)$.

It is supposed that the motion of this mass point through space can be described by a one-parameter family (in time) of locations considered to be continuous and sufficiently differentiable to allow the following deformation gradients to be defined

$$F_{ij}(t_0, t) = \frac{\partial x_i}{\partial X_j}, \quad \hat{F}_{ij}(s, t) = \frac{\partial x_i}{\partial \chi_j}, \quad \tilde{F}_{ij}(t_0, s) = \frac{\partial \chi_i}{\partial X_j}, \quad (1)$$

where indices i and j have values 1, 2, 3. Here these formulæ have been written in component form; in tensor notation they are written as

$$\mathbf{F} = F_{ij} \mathbf{e}_i \otimes \mathbf{e}_j, \quad \hat{\mathbf{F}} = \hat{F}_{ij} \mathbf{e}_i \otimes \mathbf{e}_j, \quad \tilde{\mathbf{F}} = \tilde{F}_{ij} \mathbf{e}_i \otimes \mathbf{e}_j, \quad (2)$$

where \otimes is the vector outer product. These fields satisfy the identity $\mathbf{F} = \hat{\mathbf{F}} \tilde{\mathbf{F}}$, or equivalently, $F_{ij} = \hat{F}_{ik} \tilde{F}_{kj}$ where the repeated k index is summed over in the usual manner. The ability to invert these fields is guaranteed by the conservation of mass.

Deformation fields are two-state fields that can be scalar, vector, or tensor valued. Hereafter, arguments denoting the state dependence of these fields are omitted for brevity, at least for the most part. Instead, as in Eq. (2), plain-symboled deformation fields are considered to have a state dependence of (t_0, t) ; hatted deformation fields are considered to have a state dependence of (s, t) ; and tilded deformation fields are considered to have a state dependence of (t_0, s) .

Affiliated with the above deformation gradients are the left- and right-deformation tensors defined by

$$\mathbf{B} = \mathbf{F} \mathbf{F}^T \quad \text{and} \quad \mathbf{C} = \mathbf{F}^T \mathbf{F}, \quad (3)$$

respectively, where ‘T’ implies transpose (viz., $B_{ij} = F_{ik} F_{jk}$ and $C_{ij} = F_{ki} F_{kj}$). By $\hat{\mathbf{B}}$ we mean $\hat{\mathbf{F}} \hat{\mathbf{F}}^T$, etc. The left-deformation tensor \mathbf{B} of Finger (1894) typically appears in Eulerian constructions, while the right-deformation tensor \mathbf{C} of Green (1841) typically appears in Lagrangian constructions.

For model implementation into numerical codes, like finite elements, it is often useful to split the deformation variables into hydrostatic and deviatoric parts. Following Flory (1961), we assign

$$J = \det \mathbf{F}, \quad \bar{\mathbf{F}} = J^{-1/3} \mathbf{F}, \quad \bar{\mathbf{C}} = \bar{\mathbf{F}}^T \bar{\mathbf{F}}, \quad \bar{\mathbf{B}} = \bar{\mathbf{F}} \bar{\mathbf{F}}^T, \quad (4)$$

so that $\det \bar{\mathbf{F}} = 1$, and therefore, $\det \bar{\mathbf{C}} = \det \bar{\mathbf{B}} = 1$, where $\det(\bullet)$ denotes the determinant. Likewise, one can define

$$\hat{J} = \det \hat{\mathbf{F}}, \quad \hat{\bar{\mathbf{F}}} = \hat{J}^{-1/3} \hat{\mathbf{F}}, \quad \hat{\bar{\mathbf{C}}} = \hat{\bar{\mathbf{F}}}^T \hat{\bar{\mathbf{F}}}, \quad \hat{\bar{\mathbf{B}}} = \hat{\bar{\mathbf{F}}} \hat{\bar{\mathbf{F}}}^T, \quad (5)$$

and

$$\tilde{J} = \det \tilde{\mathbf{F}}, \quad \tilde{\bar{\mathbf{F}}} = \tilde{J}^{-1/3} \tilde{\mathbf{F}}, \quad \tilde{\bar{\mathbf{C}}} = \tilde{\bar{\mathbf{F}}}^T \tilde{\bar{\mathbf{F}}}, \quad \tilde{\bar{\mathbf{B}}} = \tilde{\bar{\mathbf{F}}} \tilde{\bar{\mathbf{F}}}^T, \quad (6)$$

so that $\det \hat{\bar{\mathbf{F}}} = \det \tilde{\bar{\mathbf{F}}} = 1$. A bar over a tensorial deformation field implies that it is isochoric (preserves volume), while a hat or a tilde placed on top of that designates the states for which it is isochoric.

3 Elasticity

Before one can construct a viscoelastic model for soft tissues, it is necessary to quantify the highly nonlinear elastic behavior that dominates soft-tissue response.

The strain-energy density per unit mass, when written for the Lagrangian frame, is governed by

$$dW = \frac{1}{2\rho_0} \text{tr}(\mathbf{S}d\mathbf{C}), \quad (7)$$

where $\text{tr}(\bullet)$ is the trace operator, while $dW(\mathbf{X}; t_0, t, dt)$ represents the work done over a time increment dt on a material element with mass density $\rho = \rho(\mathbf{x}; t)$, where $\rho_0 = \rho(\mathbf{X}; t_0)$. It follows that $\rho_0/\rho = \det \mathbf{F}$ from the conservation of mass. Work is caused by an imposed displacement acting on the mass element, manifested here as the strain increment $(1/2)d\mathbf{C}(\mathbf{X}; t_0, t, dt)$. The material responds to this displacement through the creation of forces, thereby producing a state of stress $\mathbf{S}(\mathbf{X}; t_0, t)$ known as the second Piola–Kirchhoff stress.

It is convenient to decompose stress into the additive sum $\mathbf{S} = \mathbf{S}_v + \mathbf{S}_d$,

where \mathbf{S}_v represents the volumetric (or spherical) contribution to \mathbf{S} , while \mathbf{S}_d represents the deviatoric (or distortional) contribution to \mathbf{S} . Hyperelasticity postulates that dW is an exact differential, and as such, Eq. (7) becomes (cf. Simo and Hughes 1998, pp. 359–361)

$$\mathbf{S}_v = \rho_0 J \frac{\partial W_v(J)}{\partial J} \mathbf{C}^{-1} \text{ and } \mathbf{S}_d = 2\rho_0 J^{-2/3} \text{Dev} \left[\frac{\partial W_d(\bar{\mathbf{C}})}{\partial \bar{\mathbf{C}}} \right], \quad (9)$$

where $\text{Dev}[\bullet] = (\bullet) - (1/3)\text{tr}[(\bullet)\mathbf{C}]\mathbf{C}^{-1}$ is the Lagrangian deviatoric operator. Here the elastic strain energy is considered to be the sum of separate volumetric W_v and deviatoric W_d parts such that $W(\mathbf{C}) = W_v(J) + W_d(\bar{\mathbf{C}})$, thereby producing like contributions to the state of stress, viz., Eq. (8). Thermodynamics also requires the potential W to depend on temperature; however, this dependency is usually ignored in tissue mechanics, and will not be introduced here.

Consider a convex pressure/volume model whose spherical strain energy is given by (Simo and Hughes 1998, pp. 361)

$$\rho_0 W_v(J) = \kappa \frac{1}{2} \left[\frac{1}{2}(J^2 - 1) - \ln J \right], \quad (10)$$

which leads to a symmetric expression for hydrostatic pressure of the form

$$p = -\kappa \frac{1}{2}(J - J^{-1}), \quad \text{or equivalently,} \\ \mathbf{S}_v = \kappa \frac{1}{2}(J^2 - 1)\mathbf{C}^{-1}, \quad (11)$$

with κ being the bulk modulus. Dilatation $(1/2)(J - J^{-1})$ is a second-order accurate approximation to the dilatation of Hencky (1928), viz., $(1/2) \ln \det \mathbf{C}$ (cf. Freed 2004).

There are two non-trivial invariants needed to describe the deviatoric response of an isotropic elastic solid (Rivlin 1948); they are:

$$I = \text{tr} \bar{\mathbf{C}} \equiv \text{tr} \bar{\mathbf{B}} \quad \text{and} \quad II = \text{tr} \bar{\mathbf{C}}^{-1} \equiv \text{tr} \bar{\mathbf{B}}^{-1}. \quad (12)$$

Consequently, the tensorial dependence of $W_d(\bar{\mathbf{C}})$ can be replaced by a scalar one of $W_d(I, II)$. The third invariant is a trivial argument, because $III = \det \bar{\mathbf{C}} = 1$ by definition. An application of the Cayley–Hamilton theorem proves the identity $III = (1/2)((\text{tr} \bar{\mathbf{C}})^2 - \text{tr}(\bar{\mathbf{C}}^2)) = \text{tr} \bar{\mathbf{C}}^{-1}$ because $\det \bar{\mathbf{C}} = 1$.

Whenever an invariant appears by itself in a strain-energy function, a *deformation tensor* ensues. Whenever the invariant sum $I + II$ appears, a *strain tensor* is produced. Desiring a strain-energy function that yields strain fields, not just deformation fields, while keeping in mind the stability constraints of Renardy (1985)⁵, we introduce a class of elastic materials whose deviatoric strain energy is described by

$$\rho_0 W_d(\bar{\mathbf{C}}) = \mu \frac{1}{4} (f(\mathbf{p}_1; I) - f(\mathbf{p}_1; 3) \\ + f(\mathbf{p}_2; II) - f(\mathbf{p}_2; 3)), \quad (13)$$

where μ is the elastic shear modulus and \mathbf{p}_i is a vector of parameters, which may have different values when associated with I and II . Function f is any function that belongs to the class of dimensionless functions which satisfies the following constraints:

$$\begin{aligned} \text{physics:} & \quad f(\mathbf{p}_1; I) \geq 0 \quad \text{and} \quad f(\mathbf{p}_2; II) \geq 0, \\ & \quad f'(\mathbf{p}_1; 3) = 1 \quad \text{and} \quad f'(\mathbf{p}_2; 3) = 1, \\ \text{monotonicity:} & \quad f'(\mathbf{p}_1; I) > 0 \quad \text{and} \quad f'(\mathbf{p}_2; II) > 0, \\ \text{convexity:} & \quad f'(\mathbf{p}_1; I) + 2If''(\mathbf{p}_1; I) > 0 \quad \text{and} \\ & \quad f'(\mathbf{p}_2; II) + 2II f''(\mathbf{p}_2; II) > 0, \end{aligned} \quad (14)$$

where $f'(x) = df(x)/dx$ and $f''(x) = d^2f(x)/dx^2$. The terms $f(\mathbf{p}_i; 3)$ in Eq. (13) are constants introduced to normalize the strain energy so that $W_d \geq 0$.

The definition for strain energy given in Eq. (13) leads to an elastic constitutive equation for the deviatoric response in the Lagrangian frame of the form

$$\mathbf{S}_d = 2\mu J^{-2/3} \frac{1}{4} \left(f'(\mathbf{p}_1; I) \text{Dev}[\mathbf{I}] - f'(\mathbf{p}_2; II) \text{Dev}[\bar{\mathbf{C}}^{-2}] \right), \quad (15)$$

where the $1/4$ is introduced so that μ corresponds with the classic definition of Lamé's elastic shear modulus in the domain of infinitesimal strains. This physical interpretation of μ applies to all models in our material class, because of the second line of constraints in Eq. (14).

An application of the pull-back operator (Holzapfel 2000, pp. 82–84) transforms the above Lagrangian formula into the following Eulerian expression

$$J\mathbf{T}_d = 2\mu \frac{1}{4} \left(f'(\mathbf{p}_1; I) \text{dev}[\bar{\mathbf{B}}] - f'(\mathbf{p}_2; II) \text{dev}[\bar{\mathbf{B}}^{-1}] \right), \quad (16)$$

where $\text{dev}[\bullet] = (\bullet) - (1/3)\text{tr}(\bullet)\mathbf{I}$ is the Eulerian deviatoric operator. The second Piola–Kirchhoff stress \mathbf{S} maps

⁵ Renardy's lemma: A sufficient condition for strong ellipticity in a K-BKZ fluid, and therefore in the deviatoric response of an isotropic elastic solid, is that its strain-energy function be strictly monotone in I and II , and strictly convex in \sqrt{I} and \sqrt{II} .

into the Cauchy stress $\mathbf{T}(\mathbf{x}; t)$ according to the well-known formula $J\mathbf{T} = \mathbf{F}\mathbf{S}\mathbf{F}^T$. Stress $J\mathbf{T}$ is called the Kirchhoff stress with $J\mathbf{T}_d$ being its deviatoric part. Strain $(1/4)(\mathbf{B} - \mathbf{B}^{-1})$ is a second-order accurate approximation of Hencky strain $(1/2) \ln \mathbf{B}$ (cf. Freed 2004).

Choosing a functional form for f that is in accordance with the constraints put forth in Eq. (14) will lead to an admissible constitutive equation for the modeling of elastic solids.

4 Viscoelasticity

Because most tissues are predominantly elastic, with a secondary viscoelastic attribute, and because the elastic response in these tissues is highly nonlinear, we believe that the K-BKZ (Kaye 1962; Bernstein et al. 1963) hypothesis⁶ has an advantage over other approaches when it comes to developing viscoelastic models for soft tissues, the most notable alternative approach being that of internal state-variable theory (Coleman and Gurtin 1967). The K-BKZ hypothesis takes the potential structure for elasticity arising from thermostatics and analytically continues it into neighboring states of irreversibility where viscoelastic phenomena can exist. The thermodynamic admissibility of this hypothesis is discussed in a separate paper by Bernstein et al. (1964).

In soft-tissue mechanics, it is reasonable to assume that only the deviatoric response is viscoelastic. There are applications where viscoelastic compressibility can be very important (cf. Leonov 1996); however, the in vivo rate-controlling relaxation mechanisms of soft tissues are not known to be affiliated with volume change.

There are two material functions that arise from the K-BKZ hypothesis. In the viscoelastic formulæ stated below, the relaxation G and memory M functions can be of whatever form one chooses. They are not specified by the construction. However, they are constrained in that $M(t-s) = \partial G(t-s)/\partial s$ and $0 \leq M(t_2) < M(t_1)$ for all $t_2 > t_1 \geq t_0$ where $G_0 = G(0) = 1$ and $G_\infty = G(\infty) = 0$, in accordance with thermodynamics through what is called the principle of fading memory (Coleman and Mizel, 1968). Examples of such functions are presented in Sect. 5.

In the Lagrangian frame, the deviatoric response that arises from an application of the K-BKZ hypothesis to the

elastic formula given in Eq. (15) leads to the constitutive equation⁷

$$\begin{aligned} \mathbf{S}_d = & 2(\mu_\infty + (\mu_0 - \mu_\infty)G(t)) \\ & \times J^{-2/3} \frac{1}{4} \left(f'(\mathbf{p}_1; \bar{\mathbf{I}}) \text{Dev}[\mathbf{I}] - f'(\mathbf{p}_2; \bar{\mathbf{I}}) \text{Dev}[\bar{\mathbf{C}}^{-2}] \right) \\ & + 2(\mu_0 - \mu_\infty) J^{-2/3} \int_{t_0}^t M(t-s) \frac{1}{4} \left(f'(\mathbf{p}_1; \hat{\mathbf{I}}) \text{Dev}[\hat{\mathbf{C}}^{-1}] \right. \\ & \left. - f'(\mathbf{p}_2; \hat{\mathbf{I}}) \text{Dev}[\bar{\mathbf{C}}^{-1} \hat{\mathbf{C}} \bar{\mathbf{C}}^{-1}] \right) ds, \end{aligned} \quad (17)$$

where μ_∞ and μ_0 are the rubbery and glassy shear-moduli, respectively. Time t_0 is associated with a stress-free equilibrium state. The invariants present in the integrand evaluate according to the formulæ $\hat{\mathbf{I}} = \text{tr} \hat{\mathbf{C}} \bar{\mathbf{C}}^{-1}$ and $\hat{\mathbf{I}} = \text{tr} \hat{\mathbf{C}} \bar{\mathbf{C}}^{-1}$.

The deviatoric state of stress associated with the Lagrangian frame \mathbf{S}_d given in Eq. (17) pushes forward into the Eulerian frame yielding

$$\begin{aligned} J\mathbf{T}_d = & 2(\mu_\infty + (\mu_0 - \mu_\infty)G(t)) \\ & \times \frac{1}{4} \left(f'(\mathbf{p}_1; \bar{\mathbf{I}}) \text{dev}[\bar{\mathbf{B}}] - f'(\mathbf{p}_2; \bar{\mathbf{I}}) \text{dev}[\bar{\mathbf{B}}^{-1}] \right) \\ & + 2(\mu_0 - \mu_\infty) \int_{t_0}^t M(t-s) \frac{1}{4} \left(f'(\mathbf{p}_1; \hat{\mathbf{I}}) \text{dev}[\hat{\mathbf{B}}] \right. \\ & \left. - f'(\mathbf{p}_2; \hat{\mathbf{I}}) \text{dev}[\hat{\mathbf{B}}^{-1}] \right) ds. \end{aligned} \quad (18)$$

This formula, representing the Eulerian version of our model, is likely to be more intuitive to the reader than its Lagrangian counterpart stated in Eq. (17). Here one would evaluate the invariants in the integrand according to the formulæ $\hat{\mathbf{I}} = \text{tr} \hat{\mathbf{B}}$ and $\hat{\mathbf{I}} = \text{tr} \hat{\mathbf{B}}^{-1}$.

Like G and M , the elastic function f is left unspecified by the general construction. It must, however, be constrained by Eq. (14) so that the deviatoric response of the model satisfies the K-BKZ stability criterion of Renardy (1985).

An integration algorithm with a unique memory management scheme has been developed by the authors (Diethelm et al., 2006) for the purpose of efficiently solving convolution integrals like those found in Eqs. (17) and (18).

5 Viscoelastic kernels

There are numerous viscoelastic kernels (a relaxation/memory function pair) that have been proposed in the literature. Here we consider five of them that have potential value in the modeling of tissues; they are: the generalized Maxwell model (GMM); the stretched exponential (KWW); the quasi-linear

⁶ Bernstein et al. (1963) state their hypothesis thusly: "For the Coleman–Noll fluid, the stress at time t depends upon the history of the relative deformation between the configuration at time t and all configurations at times prior to t . To this idea we add the following notions: (1) The effect of the configuration at time $\tau < t$ on the stress at time t is equivalent to the effect of stored elastic energy with the configuration at time τ as the preferred configuration. The effect depends on $t - \tau$, the amount of time elapsed between time τ and time t . (2) The stress at time t is the sum (integral) of all the contributions from all $\tau < t$ In effect, we are taking the concept of a strain energy function associated with the theory of finite elastic deformations, which is formulated in terms of a preferred configuration, and incorporating it in a fluid theory of the Coleman–Noll type by treating all past configurations as preferred configurations."

⁷ The formulæ listed in Eqs. (17) and (18) were derived in the body tensor formalism of Lodge (1964), and were then mapped into the Eulerian and Lagrangian spatial frames, respectively. A direct consequence of Lodge's field transfer operator is that the resulting spatial formulæ are invariant of frame. At the request of a reviewer, these derivations have been omitted to save space.

viscoelastic model (QLV); the fractional-order viscoelastic model (FOV); and a regularized fractional-derivative model (RFD). The first three are well known, the fourth is known, but apparently not to the biomechanics community, and although the fifth has been used before, we shall demonstrate that it arises from a certain regularization of the fractional derivative.

5.1 GMM kernel

The eminently popular Maxwell model (MM) has the generalized relaxation function of a decaying exponential

$$G(t) = \exp\left(-\frac{t}{\tau}\right), \quad (19)$$

whose memory function is simply

$$M(t) = \frac{\exp(-t/\tau)}{\tau}, \quad (20)$$

with material constant τ (> 0) being called the characteristic time.

The GMM is composed of a finite sum of N discrete MM elements such that

$$G(t) = \sum_{n=1}^N c_n \exp\left(-\frac{t}{\tau_n}\right),$$

$$\sum_{n=1}^N c_n = 1, \quad 0 < \tau_1 < \tau_2 < \dots < \tau_N, \quad (21)$$

whose memory function is therefore

$$M(t) = \sum_{n=1}^N \frac{c_n}{\tau_n} \exp\left(-\frac{t}{\tau_n}\right), \quad (22)$$

where each term in the sum can be thought of as being associated with a discrete integral. The sum over all c_n equaling 1 enforces $G_0 = 1$, while $G_\infty = 0$ follows if $\tau_n > 0$ for all n ; hence, GMM obeys the principle of fading memory under these pretenses.

Generalized Maxwell model is the kernel that arises from a system of first-order differential equations describing viscoelasticity when derived from the theory of internal-state variables, with there being N internal variables (cf. Simo and Hughes 1998, Chap. 10).

Any completely monotonic relaxation function, i.e., $(-1)^n d^n G(t)/dt^n \geq 0$ for all $n = 0, 1, 2, \dots$, possesses a continuous relaxation spectrum H , which is defined as the forcing function in the convolution integral $G(t) = \int_0^\infty e^{-t/\tau} H(\tau) d\tau$.⁸ Over a specified time or frequency range, such a relaxation function can be approximated by a discrete relaxation spectrum via the GMM kernel. Fulchiron et al. (1993) and Simhambhatla and Leonov (1993) propose using a Padé–Laplace technique to obtain optimum GMM parameters, where a Padé expansion of chosen order is fit to data in the Laplace domain wherein the problem becomes

⁸ Kernels KWW, QLV, FOV and RFD all have completely monotonic relaxation functions.

well posed. The results are then transformed back into the time domain for use. As a rule of thumb, about one Maxwell chain is required for each decade of frequency response that is specified by the particular boundary-value problem to be solved.

Without exception (to our knowledge), GMM is the only viscoelastic kernel preprogrammed into commercial finite element codes that have viscoelastic material models bundled with them.

5.2 KWW kernel

A popular relaxation function from the viscoelastic liquids literature is the stretched exponential of Kohlrausch (1847) and Williams and Watts (1970) (KWW), which for a solid is given by

$$G(t) = \exp\left(-\left(\frac{t}{\tau}\right)^\beta\right), \quad (23)$$

whose memory function is therefore

$$M(t) = \frac{\beta \exp\left(-\left(\frac{t}{\tau}\right)^\beta\right)}{t^{1-\beta} \tau^\beta}, \quad (24)$$

where τ (> 0) and β ($0 < \beta \leq 1$) are the material constants.

This relaxation function is normalized in the sense that $G_0 = 1$ and $G_\infty = 0$. The memory function is singular at the origin, i.e., $M_0 = \infty$ (given $0 < \beta \leq 1$), with $M(t)$ monotonically asymptoting towards $M_\infty = 0$ with increasing t . However, if β were allowed to be greater than 1, then $M_0 = M_\infty = 0$ and the memory function would no longer be monotonic, violating the principle of fading memory. Consequently, $0 < \beta \leq 1$ in order for Eqs. (23) and (24) to be in accordance with this physical principle.

5.3 QLV kernel

Quasi-linear viscoelasticity (QLV) was introduced into the biomechanics literature by Fung (1971), with its relaxation function not appearing until much later (Fung 1993, pp. 285). When written as a generalized relaxation function, it becomes

$$G(t) = \frac{E_1(t/\tau_2) - E_1(t/\tau_1)}{\ln(\tau_2/\tau_1)}, \quad (25)$$

with parameters τ_1 (> 0) and τ_2 ($> \tau_1$) designating material constants, wherein

$$E_n(x) = \int_1^\infty y^{-n} e^{-xy} dy \quad (26)$$

is the exponential integral. The QLV relaxation function satisfies $G_0 = 1$ and $G_\infty = 0$. The memory function associated with this relaxation function is more user friendly, it being simply

$$M(t) = \frac{\exp(-t/\tau_2) - \exp(-t/\tau_1)}{t}. \quad (27)$$

QLV has become the de facto standard for characterizing soft-tissue viscoelasticity in the biomechanics literature.

The QLV relaxation function is not usually written in the above format. Specifically, the rubbery modulus μ_∞ does not appear in the QLV literature; rather, a parameter c (> 0) appears that relates the glassy modulus μ_0 to the rubbery modulus via $\mu_\infty = \mu_0/[1 + c \ln(\tau_2/\tau_1)]$, where c represents the height of a box relaxation spectrum that begins at time τ_1 and ends at time τ_2 . Because $M_0 = 1/\tau_1 - 1/\tau_2$ is positive, with $M(t)$ monotonically decreasing to 0 as $t \rightarrow \infty$, the QLV kernel is found to be in accordance with the principle of fading memory.

Puso and Weiss (1998) used the GMM kernel, employing seven MM kernels, to discretize the QLV kernel so that they could approximate QLV for implementation into a commercial finite element code.

5.4 FOV kernel

Caputo and Mainardi (1971a,b) analytically continued the standard viscoelastic solid (Zener 1948, pp. 43)

$$[1 + \tau D]\sigma(t) = E_\infty[1 + \rho D]\epsilon(t),$$

$$\sigma_{0+} = E_\infty \left(\frac{\rho}{\tau}\right) \epsilon_{0+}, \quad (28)$$

by replacing its derivatives in time $Df(t) = \partial f(t)/\partial t$ with the Caputo (1967) fractional derivative of order α in time (cf. Podlubny 1999, pp. 78–81)

$$D_\star^\alpha f(t) = \frac{1}{\Gamma(1-\alpha)} \int_{t_0}^t \frac{Df(s)}{(t-s)^\alpha} ds, \quad 0 < \alpha < 1, \quad t > t_0, \quad (29)$$

thereby producing the constitutive equation

$$[1 + \tau^\alpha D_\star^\alpha]\sigma(t) = E_\infty[1 + \rho^\alpha D_\star^\alpha]\epsilon(t),$$

$$\sigma_{0+} = E_\infty \left(\frac{\rho}{\tau}\right)^\alpha \epsilon_{0+}, \quad (30)$$

that we call the (Kelvin–Zener) FOV solid⁹, which becomes the standard viscoelastic solid listed in Eq. (28) whenever $\alpha = 1$. Variables σ and ϵ represent engineering stress and strain, respectively, with $\sigma_{0+} = \sigma(t_{0+})$ and $\epsilon_{0+} = \epsilon(t_{0+})$ specifying their initial conditions at time t_{0+} ($= t_0 + \varepsilon$, where ε is a small positive number). This 1D model has four material constants: E_∞ (> 0) denotes the rubbery elastic modulus, α ($0 < \alpha < 1$) is the fractional order of evolution, τ (> 0) represents the characteristic relaxation time, and ρ ($> \tau$) is the characteristic retardation time, with $E_0 = (\rho/\tau)^\alpha E_\infty$ ($> E_\infty$) establishing the glassy elastic modulus. See Mainardi

⁹ The Voigt FOV solid is defined by

$$\sigma(t) = E[1 + \rho^\alpha D_\star^\alpha]\epsilon(t),$$

while the (Maxwell) FOV fluid is defined by

$$[1 + \tau^\alpha D_\star^\alpha]\sigma(t) = \eta^\alpha D_\star^\alpha \epsilon(t), \quad \sigma_{0+} = \left(\frac{\eta}{\tau}\right)^\alpha \epsilon_{0+},$$

where η is the viscosity, and now $E_\infty = 0$.

(2002) for an overview on the use of the fractional calculus in linear viscoelasticity.

An analytic solution to the FOV solid (Eq. 30) was obtained by Caputo and Mainardi (1971a) through an application of the method of Laplace transforms. They were able to apply this technique to Eq. (30) because it is a linear differential equation, albeit of fractional order. The solution they arrived at is a special case of Boltzmann (1874) viscoelasticity

$$\sigma(t) = E_\infty \epsilon(t) + (E_0 - E_\infty) \left(G(t) \epsilon_{0+} + \int_{t_0}^t G(t-s) \frac{\partial \epsilon(s)}{\partial s} ds \right), \quad (31)$$

where the FOV relaxation function is determined to be

$$G(t) = E_{\alpha,1} \left(-\left(\frac{t}{\tau}\right)^\alpha \right), \quad (32)$$

with

$$E_{\alpha,\beta}(t) = \sum_{k=0}^{\infty} \frac{t^k}{\Gamma(\beta + \alpha k)}, \quad \alpha > 0, \quad (33)$$

defining the two-parameter Mittag–Leffler function (cf. Podlubny 1999, pp. 16–37). Equation (32) satisfies the constraints $G_0 = 1$ and $G_\infty = 0$. The Mittag–Leffler function first appeared as a relaxation function in the paper of Gross (1947), where it was introduced in an attempt to remedy inconsistencies present in the power-law creep function. Gross did not connect the Mittag–Leffler relaxation kernel with the fractional calculus. That took place later in the papers of Caputo and Mainardi (1971a,b).

After an integration by parts and an application of the additivity of infinitesimal strains (i.e., $\epsilon(t_0, t) = \epsilon(t_0, s) + \epsilon(s, t)$ for all $s \in [t_0, t]$), Boltzmann's viscoelastic model (31) becomes

$$\sigma(t) = (E_\infty + (E_0 - E_\infty) G(t)) \epsilon(t_0, t) + (E_0 - E_\infty) \int_{t_0}^t M(t-s) \epsilon(s, t) ds, \quad (34)$$

where now the reference state is s in the strain variable that lies under the integral sign. This is consistent with the physical notion that interval $[s, t]$ constitutes that part of the deformation history which the material recollects, while the preceding interval $[t_0, s]$ represents that part of the history which the material has forgotten. Equation (34) is the small-strain 1D version of Eqs. (17) and (18).

The FOV memory function applicable to Eq. (34) is

$$M(t) = -\frac{E_{\alpha,0} \left(-(t/\tau)^\alpha \right)}{t}, \quad (35)$$

where, notably, $E_{\alpha,0}(x)$ appears in the memory function, while $E_{\alpha,1}(x)$ appears in the relaxation function. The derivative $dE_{\alpha,\beta}(x)/dx$, which is required because of $M(t-s) = \partial G(t-s)/\partial s$, can be found in Podlubny (1999, pp. 22), for

example. This memory function also appeared in the paper of Gross (1947), but it was written as $-dE_\alpha(-(t/\tau)^\alpha)/dt$, where $E_\alpha(x) \equiv E_{\alpha,1}(x)$ is the one-parameter Mittag–Leffler function (wherein $\beta = 1$). Gross did not make use of the two-parameter Mittag–Leffler function $E_{\alpha,\beta}(x)$. The FOV memory function has not reappeared in the viscoelastic literature since its introduction some 60 years ago.

One needs to be careful to distinguish between the Mittag–Leffler function $E_{m,n}(x)$ (especially the one-parameter Mittag–Leffler function $E_n(x)$) and the exponential integral $E_n(x)$, all of which are their accepted notations.

Relaxation functions described in terms of the Mittag–Leffler function, as occur in phenomenological FOV models, arise naturally from the statistical mechanics of random walks made with steps taken at random intervals (Douglas 2000). Exponential relaxation occurs whenever the steps are taken at a uniform interval in time.

In the thesis of Adolfsson (2003, paper 1), the Voigt FOV relaxation spectrum was discretized to obtain analytic formulae for the Maxwell chain coefficients c_n given that $\tau_n = n\tau/N$, $n = 1, 2, \dots, N$, with τ being the characteristic relaxation time from the Voigt FOV model. For a value for α of 0.67 (typical of synthetic polymers) he found that the normalized relaxation function predicted by 10,000 MM elements to be in about 1% error with that of the Voigt FOV relaxation function, the relaxation function obtained by using 1,000 MM elements to be in about 2% error, and when 100 MM elements were used it was in about 5% error. This demonstrates a clear advantage of the FOV kernel over the GMM kernel, provided that the FOV kernel is the ‘correct’ kernel for a given material.

Doehring et al. (2004) applied the QLV and FOV kernels to stress relaxation and cyclic data obtained from heart-valve tissues, and found their errors in predictive capability to be similar. FOV had an advantage over QLV in their parameter estimation, as only two of QLV’s three parameters were observed to be sensitive to the data. Parameter τ_2 was found to be insensitive, at least to relaxation data. This is a well-known fault of QLV. However, we did not experience this difficulty when fitting the relaxation data for the heel pad discussed in Sect. 6, as τ_2 was found to lie within the time interval of the relaxation experiment.

The authors (Diethelm et al., 2002, 2004, 2005) have developed a numerical method capable of solving the fractional differential equation found in Eq. (30).

5.5 RFD kernel

Single-integral finite-strain (SIFS) viscoelasticity (Johnson et al. 1996) employs a relaxation function of the type $G(t) = \delta/(\delta + t)$ that can be analytically continued as a power law so that the relaxation function becomes

$$G(t) = \left(\frac{\delta}{\delta + t} \right)^\alpha, \tag{36}$$

whose affiliated memory function is just

$$M(t) = \frac{\alpha \delta^\alpha}{(\delta + t)^{\alpha+1}}, \tag{37}$$

where $\alpha (> 0)$ and $\delta (> 0)$ are the material constants. Williams (1964) was the first to use this kernel, where it was used to describe the relaxation behavior of solid rocket propellants. He called it the modified power law.

Here $G_0 = 1$ and $G_\infty = 0$, as required, and $M_0 = \alpha/\delta$ with $M(t)$ monotonically decreasing toward $M_\infty = 0$, thereby ensuring that RFD possesses a fading memory kernel.

This kernel is not an Abel kernel, although it is similar in many respects. Specifically, Eq. (36) is not the Voigt FOV kernel $G(t) = t^{-\alpha}/\Gamma(1 - \alpha)$ associated with the fractional derivative in Eq. (29). In the Voigt FOV kernel, $G_0 = \infty$ and $G_\infty = 0$, and therefore, the derivative is singular at the upper limit of integration. Rather, Eq. (36) is a kind of *regularized fractional derivative* (RFD) kernel whose relaxation function G is normalized so that $G_0 = 1$. This is accomplished by pushing the singularity outside the interval of integration by a small distance δ (relative to t) so that Caputo’s derivative, Eq. (29), for $0 < \alpha < 1$, is regularized in the sense that

$$D_\delta^\alpha f(t) = \frac{1}{\Gamma(1 - \alpha)} \int_{t_0}^t \frac{Df(s)}{(t + \delta - s)^\alpha} ds, \tag{38}$$

$\delta > 0, \quad \delta/(t - t_0) \ll 1,$

where the singularity is moved to $t + \delta$. The Voigt FOV kernel and the RFD kernel are indistinguishable at large t . It is only when $t < \delta$ that these two kernels differ significantly. Exponent α can therefore be interpreted as a fractional order of evolution. Similarities and differences between the Voigt FOV and RFD kernels have been quite thoroughly investigated by Bagley (1987).

The RFD kernel is not the only way in which a fractional derivative can be regularized. Two alternative methods have been proposed in the mathematical literature. The first one, completely different from the modified power law of RFD, is based on a discretization of the fractional derivative—see, e.g., Tuan and Gorenflo (1994a,b). The second one, described by, e.g., Rubin (1996, Sect. 11) or Gorenflo and Rubin (1994), is much closer to, but not identical with the RFD concept. Their method to tackle the singularity in the Voigt kernel mentioned above is very simple: Instead of using the full (and singular) integration range from t_0 to t in the definition of the Caputo derivative, Eq. (29), they only integrate from t_0 to $t - \delta$ with a certain (positive but small) regularization parameter δ , thus cutting off the part of the interval where the singularity appears; it still occurs at time t . Compared to our approach, their method has the charm that the correspondence between the kernel $(t - s)^{-\alpha}$ and the forcing function $f(s)$ remains unchanged, whereas, our scheme shifts one factor by an amount of δ but does not shift the other factor simultaneously. This feature seems to be an advantage of the method of Gorenflo and Rubin. On the other hand, their cut-off strategy means that in an actual computation of the fractional derivative, which is supposed to be

a functional with full but fading memory, the contribution that is associated with the most recent past (the time interval from $t - \delta$ to the current time t) is ignored completely; but our method retains this information.

In this section, we have introduced five different viscoelastic kernel functions. Answering the question ‘‘Which kernel function is best for a given material?’’ is the subject of the next section.

6 Akaike information criterion

‘‘Truth in the biological sciences and medicine is extremely complicated, and we cannot hope to find exact truth or full reality from the analysis of a finite amount of data. Thus, inference about truth must be based on a good approximating model. Likelihood and least squares methods provide a rigorous inference theory if the model structure is ‘given.’ However, in practical scientific problems, the model is *not* ‘given.’ Thus, the critical issue is, ‘what is the best model to use.’ This is the model selection problem.’’ (Burnham and Anderson 2002, pp. 47)

We have used theory to provide mathematical (tensorial) structure to a class of material models that contains a known (finite) set of candidates. However, theory is unable, at least in our case, to discern which candidate model is ‘best’, especially since our models are nonlinear. We therefore desire a methodology whose outcome will *objectively* select the best model from this set of candidate models when fit against known data prone to noise. We refrain from *subjectively* assigning the model, which is accepted practice in the biomechanics literature of today. Instead, we employ the AIC – a technology for use in model selection via multi-model inference. Other criteria also exist (see, e.g., Burnham and Anderson 2002, pp. 65–70). AIC is based on the principle of parsimony: a compromise between bias-squared (simplicity: increases with decreasing numbers of model parameters) and variance (complexity: increases with increasing numbers of model parameters). AIC uses maximum log-likelihood inference to obtain ‘optimum’ parameter estimates for each candidate model. These estimates, in conjunction with the objective function, are then inputs into a Kullback–Leibler (KL) information-theoretic that is used to discern the ‘best’ model for inference, selected from the set of fitted models. The selected ‘best model’ need not be the ‘model that fits best’.

Consider an optimization problem where:

- K is the number of candidate models,
- L is the dimension of unknown parameters $\mathbf{p} = [p_1, p_2, \dots, p_L]^T$,
- M is the dimension of state variables $\mathbf{y} = [y_1, y_2, \dots, y_M]^T$, and
- N is the number of observed variables $\mathbf{y}^i = [y_1^i, y_2^i, \dots, y_M^i]^T$, $\{t_i; y_j^i\}_{j=1:M}^{i=1:N}$, with t_i being the associated times of observation.

Consider the special case where:

1. errors between observations \mathbf{y}^i and \mathbf{y}^{i+1} are independent $\forall i \in \{1, \dots, N-1\}$,
2. errors in observations \mathbf{y}^i are normally distributed about the solution $\mathbf{y}(t_i, \hat{\mathbf{p}})$, with $\hat{\mathbf{p}}$ being the optimum parameters,
3. errors between y_k^i and y_ℓ^i are independent for all $k \neq \ell$ over all the i , and
4. a constant coefficient of variation exists in the observations y_j^i , which is independent of j over all the i .

If the above conditions hold, then Baker et al. (2005) have shown that the maximum log-likelihood estimate reduces to a weighted least-squares estimate whose weights are elements from the inverse of the covariance matrix of errors, which permits a dimensionless objective function to be defined as

$$\Phi(\mathbf{p}) = \sum_{i=1}^N \sum_{j=1}^M \left(\frac{y_j(t_i, \mathbf{p}) - y_j^i}{y_j^i} \right)^2, \quad (39)$$

implying a least-squares coefficient of variation of $\sigma = 1$; whereas, the maximum likelihood estimate for the coefficient of variation in the data is given by

$$\sigma^2 = \frac{1}{MN} \Phi(\hat{\mathbf{p}}). \quad (40)$$

Akaike’s (cf. Burnham and Anderson 2002, pp. 60–64) measure for multi-model inference is then quantified via

$$\mu_{\text{AIC}} = MN \ln(\Phi(\hat{\mathbf{p}})) + 2(L+1) + \frac{2(L+1)(L+2)}{MN-L-2}, \quad (41)$$

wherein the $\Phi(\mathbf{p})$ of Eq. (39) has been minimized to get the maximum likelihood estimates $\hat{\mathbf{p}}$ for the model parameters, whose dimension L may vary from model to model; however, dimensions M and N remain fixed. The last two terms on the right-hand side of μ_{AIC} correct for model bias in the sense of KL information theory. The ‘best’ model for the purpose of inference is the one with the smallest or most negative μ_{AIC} .

Confidence intervals can be assigned to each parameter \hat{p}_ℓ in $\hat{\mathbf{p}}$. If we denote $\tilde{\mathbf{p}}_\ell = [\hat{p}_1, \hat{p}_2, \dots, \hat{p}_{\ell-1}, \tilde{p}_\ell, \hat{p}_{\ell+1}, \dots, \hat{p}_L]^T$ such that $\tilde{p}_\ell \in [p_\ell^{\min}, p_\ell^{\max}] (\chi_1^2)$, then confidence intervals are obtained by (Venzon and Moolgavkar 1988)

$$MN |\ln(\Phi(\tilde{\mathbf{p}}_\ell)) - \ln(\Phi(\hat{\mathbf{p}}))| \leq \chi_1^2, \quad (42)$$

wherein χ_1^2 is the χ^2 -distribution for one degree of freedom, which for the 0.95 quantile is 3.841, for example. $\Phi(\tilde{\mathbf{p}}_\ell)$ varies only parameter p_ℓ from optimum $\hat{\mathbf{p}}$ in a search for those values p_ℓ^{\min} and p_ℓ^{\max} that will satisfy the equality in Eq. (42).

For a given data set, a ‘best’ model can be obtained by employing the straightforward methodology outlined above. But will this model be the ‘best’ for another data set? Maybe not. Rules have been developed that allow one to dismiss those models that are not likely to ever be ‘best’, while retaining a subset of ‘good’ models. Begin by constructing the AIC differences

$$\Delta_i = \mu_{\text{AIC}_i} - \min_{k=1}^K \mu_{\text{AIC}_k}. \quad (43)$$

One then applies the following rule to infer which models are ‘good’, which are ‘mediocre’ and which are ‘poor’ (Burnham and Anderson 2002, pp. 70):

Table 1 Optimized parameters μ_{qs} , μ_{dyn} , n_1 , and n_2 for the quasi-static and dynamic elastic responses of the human calcaneal fat pad in unconfined compression, cf. Figs. (1) and (2)

$f'(x)$	μ_{qs} (kPa)	μ_{dyn} (kPa)	n_1	n_2	Φ	σ	μ_{AIC}	Δ_i
x^n	0.691	2.214	2.59	$n_2 = n_1$	5.5662	0.2395	175.0	0
x^n	0.685	2.177	5.08	1.29	5.5414	0.2390	176.7	1.7
e^{nx}	0.700	2.274	0.708	$n_2 = n_1$	5.6306	0.2409	176.1	1.1
e^{nx}	0.692	2.227	1.40	0.405	5.5722	0.2397	177.3	2.3

Δ_i	Level of empirical support for model i
0–2	Good model
4–7	Mediocre model
> 10	Poor model

It is not the absolute size of the AIC measure μ_{AIC} that matters, but rather, it is the relative value of the AIC difference Δ_i that is important. The above rule is based on the weight of evidence in favor of model i being the actual KL ‘best’ model for the problem at hand, given that one of the candidate models is actually this model; in other words, this rule has a solid footing in information theory.

7 Human calcaneal fat pad

Soft tissues are comprised primarily of water, whose bulk modulus is 2.2 GPa. Most of these tissues have shear moduli that typically range from a kPa to hundreds of MPa. Consequently, the ratio of their bulk to shear moduli usually lies between 10 and 100,000, depending on the tissue. For the fat pad of the heel, this ratio is about 100,000, making incompressibility an excellent assumption to impose for this tissue.

7.1 Elastic behavior

Few tissues in the human body are isotropic. The calcaneal fat pad in our feet has been demonstrated via experiment to be isotropic (Miller–Young 2003). This makes the heel pad an ideal tissue to work with for the purpose of deciphering mathematical structure, and to assess capability of the AIC information theoretic in model selection through multi-model inference. Extending the structure of our model to anisotropic tissues is a topic for future work.

There are a variety of functional forms for f that one could investigate which will satisfy the constraints laid down in Eq. (14). We shall consider four models constructed from the following two mathematical functions:

$$\begin{aligned} f(x) &= \frac{1}{n+1}x^{n+1}, \quad n > 0, \quad x \in \{I/3, II/3\}, \\ f(x) &= \frac{1}{n}e^{nx}, \quad n > 0, \quad x \in \{I-3, II-3\}. \end{aligned} \quad (44)$$

Parameter μ is common to all models, while the parameter vectors \mathbf{p}_i are equal (i.e., $\mathbf{p}_1 = \mathbf{p}_2 = \{n\}$) in two of the models, and distinct (viz., $\mathbf{p}_1 = \{n_1\}$ and $\mathbf{p}_2 = \{n_2\}$) in the other two models. The power law has a long history in tissue mechanics, dating back to Mitton (1945), but more prominent in the biomechanics literature of today is the exponential law advocated by Fung (1967).

We proceed by acquiring maximum log-likelihood estimates for the unknown material parameters in each of the four candidate models, along with a suite of statistical parameters: the objective function Φ , the coefficient of variation in the data σ , the AIC information theoretic μ_{AIC} and the AIC difference Δ_i ; all defined in Sect. 6. These values have been tabulated in Table 1. Quasi-static and dynamic experiments were fit simultaneously—see Figs. 1 and 2. It was postulated and verified that only the shear modulus μ exhibits a rate dependence, whereas n is rate insensitive in a statistical sense, which is why there are two shear moduli reported in Table 1; they are the shear moduli belonging to these two experiments, and are not to be confused with the viscoelastic rubbery μ_∞ and glassy μ_0 shear moduli introduced in Sect. 4.

By employing the methodology from information theory presented in Sect. 6, an examination of the data presented in Table 1 allows one to conclude that the power-law and exponential models are both ‘good’ candidates for the modeling of unconfined compression in the human heel pad, with the power-law being only slightly better in this instance. The power law has an additional practical advantage over the exponential in that it is more efficient and robust in a finite element setting. For both function types, the models with $n_1 = n_2$ were found to be superior to their affiliated models where $n_1 \neq n_2$. The additional parameter present in the models where $n_1 \neq n_2$ brought no added value to these models from the perspective of information theory,

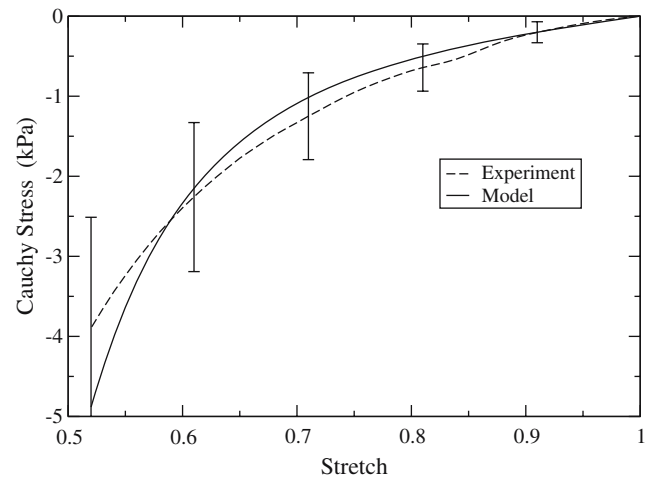


Fig. 1 Quasi-static stress/stretch response to 50% deformation at $\dot{\lambda} = -10^{-3} \text{ s}^{-1}$. Experimental mean and standard deviation data (obtained from 10 feet) are from Miller–Young (2003)

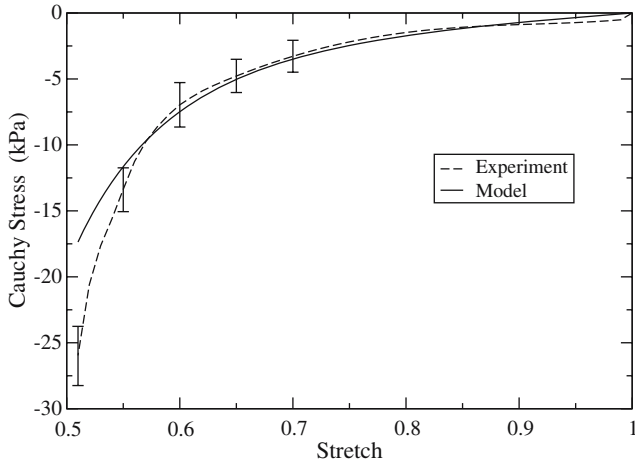


Fig. 2 Dynamic stress/stretch response to 50% deformation at $\dot{\lambda} = -35 \text{ s}^{-1}$. Experimental mean and standard deviation data (obtained from 7 feet) are from Miller–Young (2003)

allowing the simpler models where $n_1 = n_2$ to be selected. Herein lies the true worth of the AIC information theoretic: models with differing numbers of material parameters can be assessed *objectively* to determine which is best. AIC provides a metric for the Kullback–Leibler (KL) information space by which distances can be measured between various mathematical models (via the AIC differences Δ_i) whose parameters are all fit against a common data set.

Fits of the power-law model (using Eqs. 16 and 44 with $n_1 = n_2$) to the quasi-static and dynamic, experimental data sets of Miller–Young et al. (2002) can be found in Figs. 1 and 2. Although not perfect, these fits are within experimental variation up to about 45% compression ($\lambda = 0.65$). There is too much curvature in the model to correlate the quasi-static data with exacting precision. In contrast, there is not enough curvature in the model to accurately correlate the dynamic data. The model should therefore provide reasonable approximations of reality over a wide range in dynamic input. Placing 95% confidence intervals around the parameters of this fit (see Eq. 42) puts $n \in [2.30, 2.85]$, while $\mu_{\text{qs}} \in [0.48, 0.90]$ kPa and $\mu_{\text{dyn}} \in [1.55, 2.89]$ kPa. These are maximum-likelihood confidence intervals, which need not be symmetric about their optimum values, as is the case with least-squares confidence intervals.

7.2 Viscoelastic behavior

Contrary to most soft-tissue testing, the experiments of Miller–Young et al. (2002) were not preconditioned. They were done in unconfined compression beginning from a state of static equilibrium, and under this boundary condition and an assumption of incompressibility, Eq. (18) simplifies to

$$T_{11} = \frac{F}{A} = \frac{\lambda F}{A_0} = 2(\mu_{\infty} + (\mu_0 - \mu_{\infty}) G(t)) \times \frac{1}{4} (f'(\mathbf{p}_1; I) (\lambda^2 - \lambda^{-1}) + f'(\mathbf{p}_2; II) (\lambda - \lambda^{-2}))$$

$$+ 2(\mu_0 - \mu_{\infty}) \int_{t_0}^t M(t-s) \frac{1}{4} (f'(\mathbf{p}_1; \hat{I}) (\hat{\lambda}^2 - \hat{\lambda}^{-1}) + f'(\mathbf{p}_2; \hat{II}) (\hat{\lambda} - \hat{\lambda}^{-2})) ds, \quad (45)$$

where $I = \lambda^2 + 2\lambda^{-1}$ and $II = 2\lambda + \lambda^{-2}$ are the invariants with λ being replaced by $\hat{\lambda}$ in \hat{I} and \hat{II} , which are arguments in f' . Here F is the applied force, A_0 and A are the initial and current cross-sectional areas, and $\lambda = \ell/\ell_0$ and $\hat{\lambda} = \ell/\ell_s$ are the two stretches present, with ℓ_0 , ℓ_s , and ℓ representing the respective initial, intermediate and current lengths of a gage section scribed to the specimen.

Because the loading history was not recorded by Miller–Young (2003) for their stress-relaxation experiment, we were forced to impose an idealized loading history. This is not desirable (Doehring et al. 2004; Gimbel et al. 2004), but it is the best one can do in this case. A deformation rate of $\dot{\lambda} = -100 \text{ s}^{-1}$ was assumed, which is in the vicinity of the uppermost capabilities of modern servo-hydraulic testing equipment. This rate was applied for 0.004 s to produce a final stretch of $\lambda = 0.6$ that was then held fixed for 1 min. This loading history allows the integral in Eq. (45) to be decomposed into the sum of two integrals. The first integral is over the interval of loading $t \in [t_0, t_1]$, and the second integral is over of the interval of relaxation $t \in [t_1, t_2]$. For this particular experiment, $t_0 = 0 \text{ s}$, $t_1 = 0.004 \text{ s}$ and $t_2 = 60 \text{ s}$. The advantage of breaking the integral into a sum of two integrals is that the second integral vanishes under the boundary conditions of stress relaxation, because $\hat{\lambda} = 1$ for all $s \in [t_1, t_2]$, and therefore, the forcing function (viz., strain from s to t) is 0 over the entire region $[t_1, t_2]$. All arguments t in the integrand of Eq. (45) remain t whenever $t > t_1$. Only the upper limit of integration gets changed from t to t_1 in the contributing integral.

Following the method of approach used to select an elastic model, first a set of candidate viscoelastic kernels was chosen, and then the AIC information theoretic was employed to down-select the better models at describing a specified experimental data set; in this case, the stress-relaxation experiment of Miller–Young et al. (2002). The set of candidate models chosen for consideration includes: FOV, GMM, KWW, QLV, and RFD, which are defined in Sect. 5.

Because the loading data were not recorded, we assigned a value of 2.6 to the exponent n in the previously selected elastic power-law function $f'(x) = x^n$ of Eq. (44), where no distinction is made between \mathbf{p}_1 and \mathbf{p}_2 , i.e., $\mathbf{p}_1 = \mathbf{p}_2 = \{n\}$. This value is in agreement with our findings from fitting the elastic data, and with the observation that it is the shear modulus μ , not the strain exponent n , that exhibits rate dependence. In all models except GMM, this leaves four parameters to be obtained via parameter estimation techniques, whose values are listed in Table 2.

Parameters in common betwixt all five models include the rubbery μ_{∞} and glassy μ_0 elastic shear moduli, and the elastic stretch exponent $n = 2.6$. Except for GMM, each kernel has a relaxation/memory function pair with two material parameters that we denote as c_1 and c_2 in Table 2. These are

Table 2 Optimized shear moduli μ_∞ and μ_0 , and viscoelastic kernel parameters denoted as c_1 and c_2 (see the body of the text for the mappings to their specific model parameters) for a stress relaxation of the human calcaneal fat pad, cf. Fig. 3

Model	μ_∞ (kPa)	μ_0 (kPa)	c_1	c_2	Φ	σ	μ_{AIC}	Δ_i
FOV	0.707	4.04	0.472	0.389	0.00143	0.0114	-50.1	3.1
KWW	0.921	4.64	0.263	0.272	0.00166	0.0123	-48.4	4.8
QLV	0.965	3.41	0.0059	31.8	0.00229	0.0144	-44.9	8.3
RFD	0.711	3.79	0.366	0.069	0.00108	0.0099	-53.2	0

not the notations that exist in Sect. 5, so here we establish their mappings and their units: for FOV, $c_1 = \alpha$ and $c_2 = \tau$ (s); for KWW, $c_1 = \beta$ and $c_2 = \tau$ (s); for QLV, $c_1 = \tau_1$ (s) and $c_2 = \tau_2$ (s); and for RFD, $c_1 = \alpha$ and $c_2 = \delta$ (s).

According to the selection criteria put forth in Sect. 6, RFD is a ‘good’ model for inference, FOV lies on the boundary between ‘good’ and ‘mediocre’, while both KWW and QLV are ‘mediocre’ models in this regard for this material. Given this fact, RFD is the model of choice. The computational effort required to evaluate the RFD kernel is less than the computational effort required to evaluate any of the other kernels – an added bonus. The ability of RFD to correlate these data is demonstrated in Fig. 3. We reiterate that this selection process is based on the a priori assigned set of candidate models, and on the experimental data set chosen to fit. Different results are likely to follow given different materials, data sets, and candidate models.

This outcome of RFD being the ‘best’ model for inference came as somewhat of a surprise to us. Our personal bias going into this exercise would have been to select the FOV kernel; this bias being based on many physically sound reasons. Biomechanicians would be apt to preselect QLV based on the biases of their backgrounds. The fact that QLV is not a good model for plantar soft tissue agrees with the recent findings of Ledoux et al. (2004). The capability of the RFD kernel, which is a generalization of the SIFS kernel proposed by Johnson et al. (1996), and the ease by which it can be com-

puted cannot be disputed. Other than around the origin, the RFD kernel is not all that different from the Abel kernel of the fractional derivative present in the Voigt FOV model, or the Mittag–Leffler kernel present in the Kelvin–Zener FOV model, but it is a lot easier to work with. In effect, the RFD kernel slides the singularity at the upper limit of integration in the Voigt FOV kernel so that it lies just outside the integral by a small distance of δ . We coined the acronym RFD from the phrase *regularized fractional derivative*, because it behaves like an Abel kernel whenever $t \gg \delta$, but it does not propagate a shock wave with infinite velocity like the Voigt FOV kernel does due to the regularization imposed on the RFD kernel, viz., $G_0 = 1$ for the RFD relaxation function.

For the RFD model, placing 95% confidence intervals around the parameters puts: $\mu_\infty \in [0.702, 0.721]$ (kPa), $\mu_0 \in [3.75, 3.83]$ (kPa), $\alpha \in [0.363, 0.369]$ and $\delta \in [0.066, 0.072]$ (s), with n fixed at 2.6 in accordance with our elastic findings. These confidence intervals are very tight when contrasted with those obtained for the elastic model. This is because of the high precision of fit attained with the relaxation data, as contrasted with the more moderate fit achieved with the compression data. The above confidence interval for μ_∞ lies within the confidence interval for μ_{qs} obtained earlier in this section, implying consistency between the data sets.

Conspicuously absent from the prior discussion is the GMM model, which is the de facto standard of the viscoelastic literature at large. The number of Maxwell chains (i.e., MM elements) considered will affect the number of material parameters present in any given GMM model. It is not uncommon in the literature to find investigators using upwards of seven to ten Maxwell elements in order to get a reasonable fit to a given set of experimental data. Nowhere, to our knowledge, has the AIC information theoretic been employed to answer the question: how many MM elements yield the ‘best’ GMM model for a given data set?

However, this very question has been asked, and answered, from the viewpoint of statistics, where the meter stick has been the minimum of some objective function. The outcome of this process is the seven to ten MM elements that are typically employed, with the actual number of Maxwell chains needed in any given instance being dependent upon the actual data being fit.

We now answer this same question using AIC as the meter stick. AIC is a marriage between statistics and information theory that enables multi-model inference. Presented in Table 3 are the maximum likelihood estimates for the parameters in three GMM models with increasing numbers

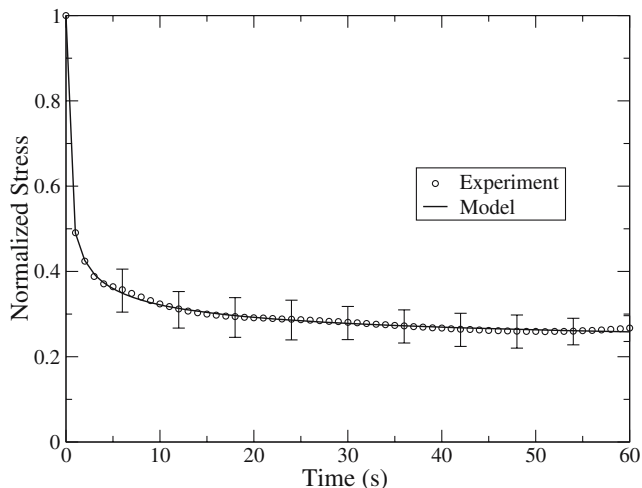


Fig. 3 Stress relaxation response at 40% deformation ($\lambda = 0.6$). Experimental mean and standard deviation data (obtained from 7 feet) are from Miller–Young (2003). The mean maximum true stress was -12.7 kPa

Table 3 Optimized parameters μ_∞ , μ_0 , τ_1 , c_2 , τ_2 , c_3 , and τ_3 for modeling stress relaxation in the human calcaneal fat pad using the GMM kernel function

MM elements	μ_∞ (kPa)	μ_0 (kPa)	c_1	τ_1 (s)	c_2	τ_2 (s)	c_3	τ_3 (s)
$N = 1$	1.12	3.45	1	1.16	–	–	–	–
$N = 2$	0.992	3.76	$1 - c_2$	0.50	0.229	10.0	–	–
$N = 3$	0.861	3.76	$1 - c_2 - c_3$	0.45	0.181	5.05	0.119	47.6

Table 4 Akaike information criterion (AIC) statistics for parameter estimates listed in Table 3

MM elements	Φ	σ	μ_{AIC}	Δ_i
$N = 1$	0.11748	0.1033	–8.9	44.3
$N = 2$	0.00233	0.0146	–33.7	19.5
$N = 3$	0.00081	0.0086	+9.6	62.8

of MM elements. Table 4 presents their associated AIC statistics. If one were to use the objective function Φ as the meter stick, or equivalently, the coefficient of variation σ , then $N = 3$ MM units would obviously be the best, and it would be better than any of the models presented in Table 2. Most likely, this could be improved upon still further by using even more MM elements. However, the AIC measure for multi-model inference μ_{AIC} overwhelmingly selects $N = 2$ as being the ‘best’ GMM model for the calcaneal fat pad. The parameters of the $N = 2$ GMM model best represent the ‘information’ present within the data amongst the various GMM models. Interestingly, this is the number of Maxwell chains used by Miller–Young (2003), where she reported values of $\tau_1 = 0.5$ s and $\tau_2 = 24$ s. We are in agreement on the former value but differ on the latter. Our differing values for τ_2 are likely due to the fact that we obtained our parameters from maximum log-likelihood estimates, whereas Miller–Young obtained hers from nonlinear regression estimates. We also employed different elastic models. Furthermore, the ramp time t_1 that she imposed in her analysis was not documented.

Comparing the best GMM model against any of the previous four models via their AIC differences Δ_i ranks the best GMM as being a ‘poor’ material model for inference according to the criteria put forth in Sect. 6.

8 Summary

An elastic strain-energy function has been proposed to have great potential for the field of tissue mechanics. An application of the AIC information theoretic led to a power-law form of this free energy as being the best choice for the purpose of describing compression in the human calcaneal fat pad. The elastic material behavior associated with this free-energy function was then analytically continued into the thermodynamically irreversible domain of viscoelasticity via the K-BKZ hypothesis. With this overall mathematical structure in hand, and with the tensorial structure that the K-BKZ hypothesis provides (as applied to our elastic strain-energy function), a new class of viscoelastic materials arises. A second application of the AIC information theoretic selected the RFD as being the best choice for the relaxation/memory func-

tion kernels present in our material model for the purpose of describing stress relaxation in the fat pads of our feet.

We have found the AIC information theoretic to be a technology of great utility in biomechanics applications, yet it is apparently an unknown technology to this discipline. It is therefore our hope that biomechanicians will find our explanation of it to be straightforward and easy to exploit. AIC provides a means whereby we can enhance our understanding of the mathematical models that we use to describe the various behaviors that tissues exhibit.

Acknowledgements Dr. Ivan Vesely, now at Childrens Hospital Los Angeles, was the PI for the project that initially supported this work. A.D.F. thanks Dr. Peter Cavanagh for his continued support after Dr. Vesely took leave from the Cleveland Clinic. We also thank: Dr. Janet Miller–Young at Mount Royal College in Calgary for supplying us with the digital data from her published experiments, Dr. Gena Bocharov from the Russian Academy of Sciences for making us aware of the AIC information theoretic and instructing us in its proper use, and Prof. Arkady Leonov from the University of Akron for making us aware of Renardy’s lemma.

References

- Adolfsson K (2003) Models and numerical procedures for fractional order viscoelasticity. PhD thesis, Chalmers University Tech., Göteborg, Sweden
- Bagley RL (1987) AIAA J 27:1412–1417
- Baker CTH, Bocharov GA, Paul CAH, Rihan FA (2005) Appl Numer Math 53:107–129
- Bernstein B, Kearsley EA, Zapas LJ (1963) Trans Soc Rheol 7:391–410
- Bernstein B, Kearsley EA, Zapas LJ (1964) J Res NBS B Math Phys 68:103–113
- Boltzmann L (1874) Sitzungsberichte der Kaiserlichen Akademie der Wissenschaften: Mathematisch-naturwissenschaftlichen Klasse, Wien 70:275–300
- Burnham KP, Anderson DR (2002) Model selection and multimodel inference: a practical information-theoretic approach, 2nd edn. Springer, Berlin Heidelberg New York
- Caputo M (1967) Geophys J Roy Astr Soc 13:529–539
- Caputo M, Mainardi F (1971a) Riv Nuovo Cimento 1:161–198
- Caputo M, Mainardi F (1971b) Pure Appl Geophys 91:134–147
- Carew EO, Doehring TC, Barber JE, Freed AD, Vesely I (2003) In: L. J. Soslowsky, T. C. Skalak, J. S. Wayne, G. A. Livesay, (eds) Proceedings of the 2003 summer bioengineering conference, ASME, New York, pp 721–722
- Cavanagh PR, Licata AA, Rice AJ (2005) Gravit Space Biol Bull 18(2):39–58

- Cavanagh PR, Valiant GA, Misevich KW (1984) In: E. C. Frederick, (ed.) Sport shoes and playing surfaces, Human Kinetics Publishers, Champaign, pp 24–46
- Chen Q, Suki B, An K-N (2004) *J Biomech Eng* 126:666–671
- Coleman BD, Gurtin ME (1967) *J Chem Phys* 47:597–613
- Coleman BD, Mizel VJ (1968) *Arch Ration Mech Anal* 29:18–31
- Diethelm K, Ford NJ, Freed AD (2002) *Nonlinear Dynam* 29:3–22
- Diethelm K, Ford NJ, Freed AD (2004) *Numer Algorithms* 36:31–52
- Diethelm K, Ford NJ, Freed AD, Luchko Yu (2005) *Comp Meth Appl Mech Eng* 194:743–773
- Diethelm K, Freed AD (2006) *Comput Math Appl* 51:51–72
- Doehring TC, Carew EO, Vesely I (2004) *Ann Biomed Eng* 32:223–232
- Douglas JF (2000) In: R. Hilfer, (ed) Applications of fractional calculus in physics. World Scientific, Singapore, pp 241–330
- Finger J (1894) *Sitzungsberichte der Akademie der Wissenschaften, Wien*, 103:1073–1100
- Flory PJ (1961) *Trans Faraday Soc* 57:829–838
- Freed AD (2004) *J Eng Mater Technol* 126:38–44.
- Fulchiron R, Verney V, Cassagnau P, Michael A, Levoir P, Aubard J (1993) *J Rheol* 37:17–34
- Fung Y-C (1967) *Am J Physiol* 213:1532–1544
- Fung Y-C (1971) In: Y.-C. Fung, N. Perrone, and M. Anliker, (eds) Biomechanics: Its foundations and objectives Prentice-Hall, Englewood Cliffs, pp 181–208
- Fung Y-C (1993) *Biomechanics: Mechanical properties of living tissues*, 2nd edn Springer, Berlin Heidelberg New York
- Gimbel JA, Sarver JJ, Soslowsky LJ (2004) *J Biomech Eng* 126:844–848
- Glöckle WG, Nonnenmacher TF (1995) *Biophys J* 68:46–53
- Gorenflo R, Rubin B (1994) *Inverse Probl* 10:881–893
- Green G (1841) *Trans Cambridge Phil Soc* 7:121–140
- Gross B (1947) *J Appl Phys* 18:212–221
- Hencky H (1928) *Z tech Phys* 9:215–220
- Holzapfel GA (2000) *Nonlinear solid mechanics: a continuum approach for engineering*, Wiley, Chichester
- Johnson GA, Livesay GA, Woo SL-Y, Rajagopal KR (1996) *J Biomech Eng* 118:221–226
- Kaye A (1962) *Non-Newtonian flow in incompressible fluids*, Technical Report 134, College of Aeronautics, Cranfield
- Kohlrausch R (1847) *Ann Phys Chem* 72:353–405
- Lang T, LeBlanc A, Evans H, Lu Y, Genant H, Yu A (2004) *J Bone Miner Res* 19:1006–1012
- Ledoux WR, Meaney DF, Hillstrom HJ (2004) *J Biomech Eng* 126:831–837
- Leonov AI (1996) *Macromolecules* 29:8383–8386
- Lodge AS (1964) *Elastic liquids: an introductory vector treatment of finite-strain polymer rheology*. Academic, London
- Mainardi F (2002) *Acoustic Interactions with submerged elastic structures Part IV* In: A. Guran, A. Boström, O. Leroy, G. Maze B: series (eds) on stability, vibration and control of systems, World Scientific, New Jersey, pp 97–126
- Miller-Young JE (2003) *Factors affecting human heel pad mechanics: A finite element study*. PhD thesis, University of Calgary, Calgary, Alberta
- Miller-Young JE, Duncan NA, Baroud G (2002) *J Biomech* 35:1523–1531
- Mitton RG (1945) *J Soc Leath Trades Ch* 29:169–194
- Oldham KB, Spanier J (1974) *The fractional calculus*. In: *Mathematics in science and engineering*, vol. 3. Academic, New York
- Podlubny I (1999) *Fractional differential equations: an introduction to fractional derivatives, fractional differential equations, to methods of their solution and some of their applications*. In: *Mathematics in science and engineering*. Academic, San Diego
- Puso MA, Weiss JA (1998) *J Biomech Eng* 120:62–70
- Renardy M (1985) *Arch Ration Mech Anal* 88:83–94
- Rivlin RS (1948) *Phil Trans R Soc London A* 241:379–397
- Rubin B (1996) *Fractional integrals and potentials*. Addison Wesley Longman, Harlow
- Simhambhatla M, Leonov AI (1993) *Rheol Acta* 32:589–600
- Simo JC, Hughes TJR (1998) *Computational inelasticity*. In: *Interdisciplinary applied mathematics*, vol. 7. Springer-Verlag, Berlin Heidelberg New York
- Suki B, Barabási A-L, Lutchen KR (1994) *J Appl Physiol* 76:2749–2759
- Tuan VK, Gorenflo R (1994) *Z Anal Anwend* 13:537–545
- Tuan VK, Gorenflo R (1994b) *Numer Func Anal Opt* 15:695–711
- Venzon DJ, Moolgavkar SH (1988) *Appl Statistician* 37:87–94
- Williams G, Watts DC (1970) *Trans Faraday Soc* 66:80–85
- Williams ML (1964) *AIAA J* 2:785–808
- Yuan H, Ingenito EP, Suki B (1997) *J Appl Physiol* 83:1420–1431
- Yuan H, Kononov S, Cavalcante FA, Lutchen KR, Ingenito EP, Suki B (2000) *J Appl Physiol* 89:3–14
- Zener C (1948) *Elasticity and anelasticity of metals*. University of Chicago, Chicago